Effects of NMR invisible oriented perturbers on signal phase

Matthew Cronin[1], Samuel Wharton[1], Anna Blazejewska[1], Penny Gowland[1], and Richard Bowtell[1]

[1] *Sir Peter Mansfield Magnetic Resonance Centre, The University of Nottingham, Nottingham, Notts, United Kingdom*

Introduction: The growing use of images based on measurements of the gradient echo signal phase in susceptibility weighted imaging and quantitative susceptibility mapping (QSM)[1], means that it is increasingly important to understand the effect of susceptibility inclusionson the measured signal phase. Generally in QSM it is assumed that the measured phase/frequency variation reflects the summed effect of the dipolar fields generated by the volume average susceptibility in each voxel. Recently, however, it has been shown that long cylindrical inclusions that generate no NMR signal have no effect on the measured signal phase when confined to a cylindrical region[2] and more generally that the phase variation produced by shaped NMR-invisible perturbers depends on their shape[3] in a short echo time regime. In these circumstances, the contribution to the average phase/frequency offset in a voxel due to the material inside the voxel does not necessarily reflect its average magnetic susceptibility. This is important because there are many examples of oriented inclusions (e.g.myelin sheaths, iron deposits and pialblood vessels), which affect the phase of the signal measured from tissues. In previous work, the effect of *randomly-oriented* spheroids on the signal magnitude and phase has been investigated in detail, including the effect of diffusion[4,5], while the effect of *oriented* spheroids has been considered to some extent, but only in the absence of diffusion[3]. Here we use numerical simulations to carry out a detailed evaluation of the effect of prolate spheroids on the signal phase.

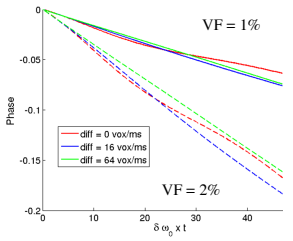

Figure 1: Phase evolution for different D-values

Theory and Methods: A prolate(needle-like) spheroid is produced by rotating an ellipse with major and minor axes of length $2c$ and $2a$ (with $c = qa$ and $q > 1$)about the c-axis. We consider single prolate spheroids of susceptibility, χ, embedded in a spherical volume, whose radius, R, is set by the desired volume fraction (VF= a^2c/R^3) of the perturbers: with the applied magnetic field, B_0, aligned with the long axis of the spheroid. The field perturbation outside the spheroid, $\delta B(\mathbf{r})$, was calculated using the expression previously described by Sukstanskii and Yablonskiy[4]. To calculate the signal evolution, 1 million "particles" were randomly seeded in the voxellatedspherical volume (R =150 voxels) , excluding the spheroid, and then each underwent a 3D random walk with time-step, δt, accumulatingposition-dependent phase,$\gamma\delta B\delta t$ at each time point. Random-walking particles were reflected at the boundary of the spheroid and particles exiting the spherical volume were randomly repositioned on the sphere's surface. The signal at each time-point was found by summing the complex signals from all particles. We focus on the summed signal's phase, ϕ, and instantaneous angular frequency, $\omega = d\phi/dt$.Simulations were carried out in Matlab, with B_0 = 7T, $\chi = 10^{-7}$ ($\delta\omega_0 = \gamma\chi B_0 = 187\ s^{-1}$) c/a= 1 (sphere), 1.5, 2, 2.5, 3 and 4, and VF = 1 or 2% (corresponding to spherical inclusions of radius 32 and 41 voxels). The diffusion rate was varied by changing the time step $\delta t = n^{-1}$ms, with n =1, 2, 4, 8, 16, 32 or 64 (D = [voxel width]^2/2δt) and simulations were also carried out with no diffusion. The time range considered was 0–0.25s, yielding a max value of $\delta\omega_0 \times t \sim 47$.

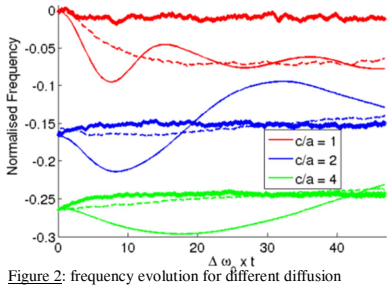

Figure 2: frequency evolution for different diffusion ratesand aspect ratios – thick lines (n =64), dashed line(n =16); continuous line (no diffusion).

Results: Figure 3 (inset) shows the imaginary part of the signal(with D= 0) in an x-$z$plane through the centre of a spheroid with c/a = 2 and VF = 2% at$t$= 0.25s, giving an indication of the form of the field variation and the extent of dephasing. Figure 2 shows the variation of the phase of the signal with $\delta\omega_0 \times t$ for spheroids with c/a = 2 and varying diffusion rates, for the two different VF's. As expected the rate of phase accumulation increases with VF, shows distinctive variation with t for no diffusion and is most affected by diffusion at longer times. Figure 3 shows the variation of scaled angular frequency, $\omega/(\delta\omega_0 \times VF)$ with $\delta\omega_0 \times t$for spheroids with varying aspect ratios and for different rates of diffusion (VF =1 %). It is evident that the frequency is dependent on the spheroid aspect ratio and shows an oscillation with time, which is damped by diffusion.

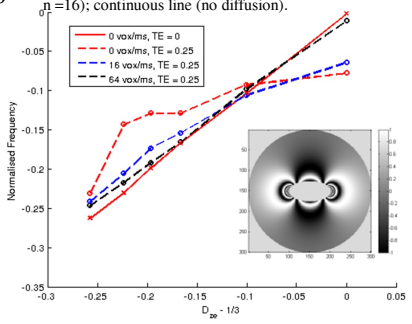

Figure 3: frequency vs D_{ze}-1/3;inset = imaginary signal map

Discussion: Three key length scales are important in the simulations: $L = 2c$ = the longest dimension of the spheroid; $L_D = \sqrt{6Dt}$ the diffusion displacement at time, t; and $L_\phi = L\sqrt[3]{\delta\omega_0 t/q^2}$ which is the radial distance from the spheroid's centre at which the phase variation due to an equivalent dipole is approximately, 2π over a spherical surface. For small $\delta\omega_0 \times t$ the average frequency depends on the average frequency offset in the volume outside the spheroid, which has previously[3] been shown to vary as $\delta\omega_0 \times VF \times (D_{ze}\text{-}1/3)$ for a spherical volume. Here, D_{ze} is the spheroid's demagnetising factor, which varies from 1/3 for a sphere to ~ 1 for a long thin needle-like spheroid. Figure 4 confirms that the scaled frequency $\omega/(\delta\omega_0 \times VF)$ at $t \sim 0$ is proportional to $(D_{ze}\text{-}1/3)$ and shows that the scaled frequency shows a similar dependence at large values of $\delta\omega_0 \times t$ for the highest diffusion rates. This also evident from Fig. 3, which shows that the frequency is time independent for the highest diffusion rate. This behaviour arises because $L_D > L$ for times when $\delta\omega_0 \times t > 2\pi$, so that the diffusion effectively averages the frequency over the volume. Oscillations of the frequency occur when L_D is not significantly larger than L_ϕ and a region of significant dephasing (where the phase varies over many multiples of π) is produced around the spheroid (Fig. 1). Although this regime was not explored in these simulations, it is expected[4] that all spheroids will produce a similar frequency offset of 0.053 $\delta\omega_0 \times VF$ when $L_\phi >> L, L_D$

Conclusion: These findings confirm that the average frequency offset produced by oriented, NMR-invisible inclusions is strongly dependent on the shape of the inclusions even in the presence of diffusion and does not therefore simply relate to the average volume susceptibility. In the short ($\delta\omega_0 \times t << 1$) and long-time ($L_D >> L, L_\phi$) regimes the frequency offset has a simple dependence on the demagnetising factor of spheroidal inclusions.

References: 1)Liu *et al.* 2009 MRM 61:196; 2) He &Yablonskiy 2009, PNAS 136, 13558; 3)Blazejewska*et al* Proc. ISMRM 2011 #4511; 4&5) Sukstanskii&Yablonskiy 2001 JMR 151: 197 & 2004 JMR 167: 56